

# Identification and quantification of components in ternary vapor mixtures using a microelectromechanical-system-based electronic nose

Weichang Zhao,<sup>1,2</sup> Lal A. Pinnaduwa,<sup>2,3,a)</sup> John W. Leis,<sup>4</sup> Anthony C. Gehl,<sup>2</sup> Steve L. Allman,<sup>2</sup> Allan Shepp,<sup>1</sup> and Ken K. Mahmud<sup>1</sup>

<sup>1</sup>*Triton Systems, Inc., 200 Turnpike Road, Chelmsford, Massachusetts 01824, USA*

<sup>2</sup>*Oak Ridge National Laboratory, P.O. Box 2008, Oak Ridge, Tennessee 37831-612, USA*

<sup>3</sup>*Department of Physics, University of Tennessee, Knoxville, Tennessee 37996, USA*

<sup>4</sup>*Department of Electrical, Electronic, and Computer Engineering, University of Southern Queensland, Toowoomba, Queensland 4350, Australia*

We report the experimental details on the successful application of the electronic nose approach to identify and quantify components in ternary vapor mixtures. Preliminary results have recently been presented [L. A. Pinnaduwa *et al.*, *Appl. Phys. Lett.* **91**, 044105 (2007)]. Our microelectromechanical-system-based electronic nose is composed of a microcantilever sensor array with seven individual sensors used for vapor detection and an artificial neural network for pattern recognition. A set of custom vapor generators generated reproducible vapor mixtures in different compositions for training and testing of the neural network. The sensor array was selected to be capable of generating different response patterns to mixtures with different component proportions. Therefore, once the electronic nose was trained by using the response patterns to various compositions of the mixture, it was able to predict the composition of “unknown” mixtures. We have studied two vapor systems: one included the nerve gas simulant dimethylmethyl phosphonate at ppb concentrations and water and ethanol at ppm concentrations; the other system included acetone, water, and ethanol all of which were at ppm concentrations. In both systems, individual, binary, and ternary mixtures were analyzed with good reproducibility.

*Author post-print of*

Zhao, W., Pinnaduwa, L., Leis, J.W., Gehl, A.C., Allman, S.L., Shepp, A. and Mahmud, K.K. (2007) *Quantitative analysis of ternary vapor mixtures using a microcantilever-based electronic nose*. *Applied Physics Letters*, 91 (4). ISSN 0003-6951, doi: 10.1063/1.2921866

## I. INTRODUCTION AND BACKGROUND

The biological nose (in particular, the canine nose) is one of the most sensitive detectors in existence today. Around a quarter of a century ago, Persaud and Dodd<sup>1</sup> realized that biological olfaction, which is highly sensitive and selective, is based on the use of multiple sensors that are only broadly selective. They proposed an “electronic nose” based on this concept.<sup>1</sup> Just as in the case of olfactory receptors,<sup>2</sup> the individual sensors in an electronic nose can only be broadly selective, since the binding of an analyte needs to be reversible. There is no requirement for an analyte-specific sensor coating; by definition, such an analyte-specific sensor would bind the analyte in a permanent way, for example, by chemisorption, and thus, it could be used only one time (a “throwaway sensor”). On the other hand, in an electronic nose, since the sensor responses are reversible, the detection can be repeated after a short recovery time. Another advantage of an electronic nose is that all of the “trained” components of the mixture are simultaneously identified and quantified.

The biological olfactory system is quite complex and highly selective. Recently, exhaustive searches of the almost complete genome sequences of human and mouse have led to the identification of around 900 odorant receptors in humans and around 1500 in mice.<sup>3</sup> The odor detection is based on the “smell” patterns generated by receptor array. The human olfactory system is able to distinguish thousands of different odors<sup>3</sup> by using pattern recognition, and some odors are due to complex mixtures of pure compounds: A particular mixture of odor molecules creates a unique response pattern in the olfactory bulb, which the brain subsequently interprets as a particular odor. At least in the initial stages, the electronic nose does not need to be that complex. In particular, detection of explosive or chemical vapors requires the identification of mostly *one or a few pure compounds*. Furthermore, some of the “interferent” vapors could be removed with the use of a preconcentrator located in front of the electronic nose. Therefore, the ability to detect a few pure compounds in simple mixtures could lead the way to a practical electronic nose for chemical and explosive vapor detection in the near future. However, by expanding the number of sensors in the sensor array, it may be possible to develop a functional electronic nose even without using a preconcentrator. To achieve such a “stand-alone” device, a microelectromechanical-system (MEMS)-based electronic nose will be required to keep the device small. It must be noted that the primary receptors in the biological nose, which are *cilia*, are comparable in size to the microcantilever sensors, and there are thousands of cilia in the biological nose.

A MEMS-based electronic nose has other highly desirable features in addition to being able to accommodate a large numbers of sensors in a small device. The rapid development of the integrated circuit technology during the past two decades has initiated the fabrication of chemical sensors on silicon or complementary metal oxide semiconductor<sup>4,5</sup>

The largely two-dimensional integrated circuit and chemical sensor structures processed by combining lithographic, thinfilm, etching, diffusive, and oxidative steps have been recently extended into the third dimension by using micromachining or MEMS technologies - a combination of special etchants, etch stops, and sacrificial layers.<sup>4</sup> Therefore, MEMS technology provides an excellent means to meet the criteria needed for a full-blown electronic nose, such as batch fabrication at low cost, low power consumption, as well as miniaturization of the devices.

Research on the development of electronic noses based on several sensor platforms has been conducted over the past two to three decades (see Refs. 6–9 and references therein). However, most effort has been devoted to the development of individual sensor coatings to achieve high sensitivity of detection. The holy grail of chemical sensors is the ability to *selectively identify target analytes*. Even though much of the work so far has been devoted to *sensitive detection of individual analytes*, any practical applications cannot be realized until *selective detection* is achieved. As mentioned

earlier, a single reversible sensor is inherently nonselective. The selectivity is to be achieved via pattern recognition based on a sensor array, just like in the case of the biological nose. Even with the increased activity in sensor array research recently, successful quantitative identification of component vapors has not been reported for mixtures with more than two components (see, for example, Refs. 10–16 and references therein). The excellent ability of a carbon black sensor array to accurately identify a number of low volatility organic molecules individually presented to the sensor array has been reported.<sup>17</sup> Similarly, a fiber optic bead-based sensor array<sup>18</sup> and microcantilever sensor array<sup>19</sup> have been shown to be able to accurately identify different odors individually presented to the sensor arrays. The most recent reports on the successful *quantitative analysis* of binary mixtures were based on surface acoustic wave sensor arrays<sup>12–14</sup> and microcantilever sensor arrays.<sup>15,16</sup> Partial success of the analysis of ternary mixtures has been described in Ref. 12, and quantitative identification of one unknown component in a ternary mixture has recently been reported.<sup>16</sup> In all these studies,<sup>8–14</sup> the concentrations of the component vapors were in the ppm range or higher.

A variety of pattern recognition algorithms has been used in conjunction with the above mentioned and other various sensor arrays (see Refs. 8 and 20–22 and references therein). Among these, the artificial neural network (ANN) mimics the mammalian neuron processing of odor stimuli, offers powerful nonlinear mapping capability and generalization ability, and is more resistant to signal noise and drift.<sup>23,24</sup> Recently, we reported a preliminary account of the detection of ppb concentrations of the nerve gas simulant dimethylmethyl phosphonate (DMMP) and ppm concentrations of ethanol and water vapor in ternary mixtures.<sup>25</sup> In this paper, we provide a detailed account of the experiments involved. *Sensitive and selective detection* of DMMP has important significance because of its relevance in the detection of chemical threats.<sup>26</sup> Furthermore, chemical sensors are notorious for their inability to deal with humidity, and this study shows that it is possible to selectively identify DMMP vapor from water vapor.

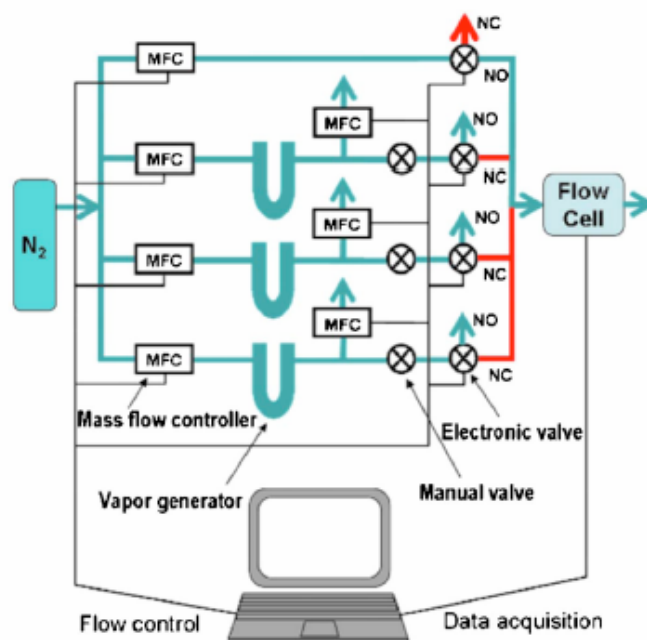


FIG. 1. (Color online) Schematic of the electronic nose system, which includes the vapor mixture generation and delivery system, the detection system (flow cell with microcantilever sensor array), and the data processing and computation system. For the electronic valves, NO is normally open and NC is normally closed.

## II. EXPERIMENTS

### A. Apparatus

A schematic diagram of the apparatus is shown in Fig. 1. There are two major parts of the apparatus: the calibrated vapor supply and the vapor detection system. The upper left part of Fig. 1 shows the vapor supply system, which is composed of mass flow controllers (MFCs), valves, vapor generators, etc., and the flow cell block in the upper right part of Fig. 1 represents the vapor detection system, which is composed of a flow cell with the microcantilever sensor array and the electronic circuit board for data acquisition. Both systems are controlled and operated by a personal computer.

The calibrated vapor supply system was designed to supply accurate, stable, and adjustable individual vapors and vapor mixtures. The system is capable of producing vapor streams with reproducibility, flexibility, and convenience in terms of concentration, mixture composition, flow rate, and vapor pulse duration. The vapors directed to the flow cell were detected by using an array of microcantilevers with different coatings to realize selective detection based on the concept of the electronic nose. Detailed descriptions on the vapor supply and the detection system will be provided below.

### B. Vapor generation and mixing

As shown in Fig. 1, there are four flow lines converging to the flow cell. The top flow line is for the supply of base flow (just the carrier gas, N<sub>2</sub>, and the other three lines are for the supply of the analyte vapors. The analyte vapors were mixed with carrier gas, N<sub>2</sub>, and diluted to low concentrations. Up to three different analyte vapors can be directed to the flow cell. The digital MFCs (Alicat Scientific) and the electronic three-way valves (Parker Hannifin) were remotely controlled by LABVIEW™ software.

The vapor generators were composed of *U*-shape holders containing diffusion vials (VICI Metronics, Inc.) of DMMP, water, ethanol, and acetone. The vials were placed in the exit side of the *U*-shape holders (three of the four vapors were available at a given time). The entrance side of the *U*-shape holder was filled with glass beads to help thermalize the carrier gas. The diffusion rate of each of the vials depends on the temperature of the liquid inside the vial and the vial's dimensions. The *U*-shape holders were immersed in temperature-controlled baths to maintain stable temperatures. In our experiments, the DMMP, water, ethanol, and acetone vapor generators were kept at 20, 10, 20, and 20 °C, respectively. The diffusion rates of the three diffusion vials were estimated by VICI Metronics to be 30, 2300, 6000, and 35 000 ng/min for DMMP, water, ethanol, and acetone, respectively. In our experiment, the flow rate of the carrier gas was kept at 50 SCCM (SCCM denotes standard cubic centimeter per minute at STP), so that the corresponding concentrations for the vapors were 100 ppb, 60 ppm, 60 ppm, and 300 ppm.

There were two flow controllers connected to each of the vapor generators. The flow controller located before a vapor generator controlled the flow rate of the carrier gas, N<sub>2</sub>, going through the vapor generator with an accuracy of 0.4% at a flow rate of 50 SCCM. The flow controller located after a vapor generator, together with a manual valve (Swagelok fine metering valve), was used to split the flow coming out of the vapor generator. One of the two split flows led to the flow cell to mix with other split flows coming from other lines. Thus, the flow through each vapor generator was maintained at a constant value (50 SCCM), while the flow rate delivered to the flow cell could be varied. The total flow rate of the vapor mixture going through the microcantilever flow cell was kept

at 50 SCCM. Therefore, while the flow rate of the mixture was kept the same as the individual flows through the vapor generators, the concentration of a component of the mixture was diluted to a factor equal to the fraction of the split flow rate to the total flow rate,

$$c_i = (\text{flow}_i/\text{flow}_t)C_i, i = 1,2,3, \quad (1)$$

where  $c_i$  is the concentration of component  $i$  in the mixture,  $\text{flow}_i$  is the flow rate of the split flow of component  $i$  to the flow cell,  $\text{flow}_t$  is the total flow rate (50 SCCM), and  $C_i$  is the concentration of the vapor  $i$  coming out of the vapor generator  $i$  (maximum concentration of vapor  $i$ ). In this report, we usually use the fraction of  $(\text{flow}_i/\text{flow}_t)$  to represent the component concentration of the mixture. We call the concentration in the unit of its maximum concentration as fractional concentration

$$F_{c_i} = (\text{flow}_i/\text{flow}_t), i = 1,2,3. \quad (2)$$

For example, if only 10 SCCM of the DMMP vapor is directed to the flow cell,  $F_{c_i}$  would be  $10/50=0.2$ , i.e., 20% of its maximum concentration; thus,  $c_i$  would be 20 ppb, since  $C_i$  was 100 ppb. The manual valves were used to build up enough gas pressure in the vapor generators required by the gas-splitting MFCs to properly work. The arrangement of the metal manual valves in the flow lines and the MFCs out of the lines allowed the flow lines to be baked.

The above design of the vapor delivery system served two major functions: (i) it allowed each vapor generator to be maintained at a constant flow rate and, thus, maintain stable vapor streams; (ii) in generating vapor mixtures, it allowed the flexibility to deliver accurate and adjustable concentrations of vapor components to the flow cell. Both of these are important to be able to consistently deliver calibrated vapor streams over long periods.

When we installed a new vapor generator to the apparatus, we always monitored the exit flow and the responses of the sensors to the vapor to make sure that there was no leaking along the line and flushed the generator with the carrier gas (N<sub>2</sub>) for several days to remove water vapor. Once a vapor generator was loaded, the carrier gas through it was kept running 24 h a day until all measurements were completed.<sup>25,26</sup>

### C. Microcantilever sensor array

The flow cell was customized to hold four Canti-4™ piezoresistive microcantilever chips (from Cation A/S, now a subsidiary of NanoNord A/S, Denmark). Each of the chips had four microcantilevers or two pairs. One cantilever of each pair was coated with gold by the manufacturer, and the other uncoated cantilever was used as a reference. We applied self-assembled monolayer (SAM) coatings to three of the chips by soaking in SAM solutions of 4-mercaptobenzoic acid (4-MBA), 2-MBA, and 4-methoxybenzenethiol. Therefore, only three different coatings were realized by those three cantilever chips. In the other chip, we applied a fresh gold coating (50 nm) on top of an existing gold-coated lever and a silver coating (50 nm) on top of the other gold-coated lever. Since the readout did not properly work for one pair of the cantilevers (coated with 4-MBA) in our experiment, the sensor array contained seven-microcantilever sensors with five different coatings. In Figs. 2–4, the sensor coatings were in the following order: 4-MBA, 2-MBA, 2-MBA, silver, gold, 4-methoxybenzenethiol, and 4-methoxybenzenethiol.

The microcantilever deflection was detected via variation of the piezo-resistance of the microcantilevers. The change in piezo-resistance of each coated microcantilever with respect to that of the reference microcantilever was measured by using a Wheatstone bridge circuit.<sup>27</sup> We selected

four Canti-4™ chips, which had best selectivity in responses to the DMMP, water, ethanol, and acetone. For example, two of the seven sensors were mainly sensitive to water vapor, two of the sensors were sensitive to water and ethanol (or acetone) but in opposite deflect directions, and one sensor was mainly sensitive to DMMP.

#### D. Measurement procedure

We studied two different vapor mixture systems by using the same seven-microcantilever array. The first was composed of DMMP, water, and ethanol (DWE mixtures) and the other was composed of acetone, water, and ethanol (AWE mixtures). Since DMMP is a nerve gas stimulant and can be detected in a relatively low concentration (100 ppb), the first mixture (DWE) was studied in more detail than the second (AWE). We usually collected one data set in 1 day. Six data sets of the DWE mixture were collected in a 2 week period, and two data sets of the AWE mixtures were collected in a 1 week period. Summaries of the DWE and the AWE mixtures are shown in Tables I and II, respectively.

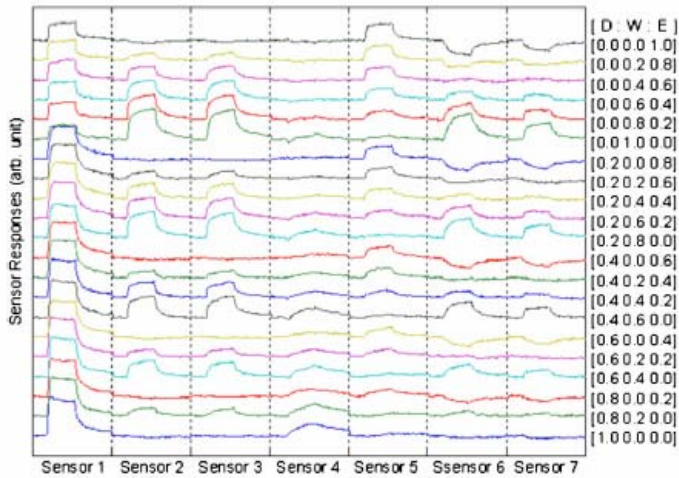


FIG. 2. (Color online) Various response patterns of the DMMP-water-ethanol vapors. The corresponding compositions are shown on the right side of the frame. There is a unique response pattern correlating to a detected composition.

Based on formula (2), the mixture composition is expressed by a three-element vector of  $(F_{C_1}, F_{C_2}, F_{C_3})$ , where  $F_{C_1} + F_{C_2} + F_{C_3} = 1$  or 100%. For example, in DWE mixtures, the three individual vapors of DMMP, water, and ethanol are expressed as (100%, 0%, 0%), (0%, 100%, 0%), and (0%, 0%, 100%), respectively, the binary mixtures are expressed with one zero fractional concentration, such as (20%, 80%, 0%), and the ternary mixtures are expressed with three nonzero fraction concentrations, such as (20%, 40%, 40%).

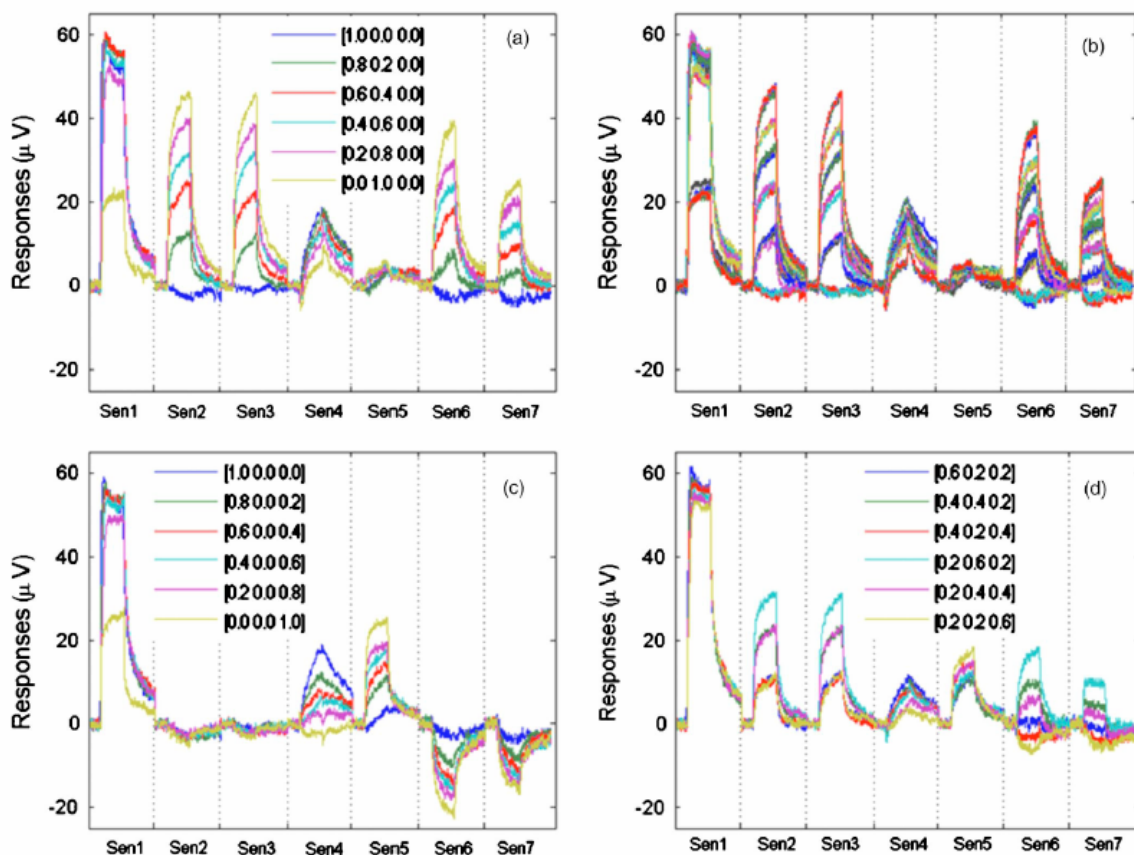


FIG. 3. (Color online) Various response patterns of the DMMP-water-ethanol vapors presented in the same level to show the distinguishable magnitudes of the responses. (a) Patterns for DMMP-water binary mixtures. (b) Patterns for the same DMMP-water binary mixtures in (a), except that there are four measured patterns to each composition to show how well the patterns were reproduced. (c) Patterns for DMMP-ethanol binary mixtures. (d) Patterns for DMMP-water-ethanol ternary mixtures. The relative compositions of the mixtures are shown in the legends.

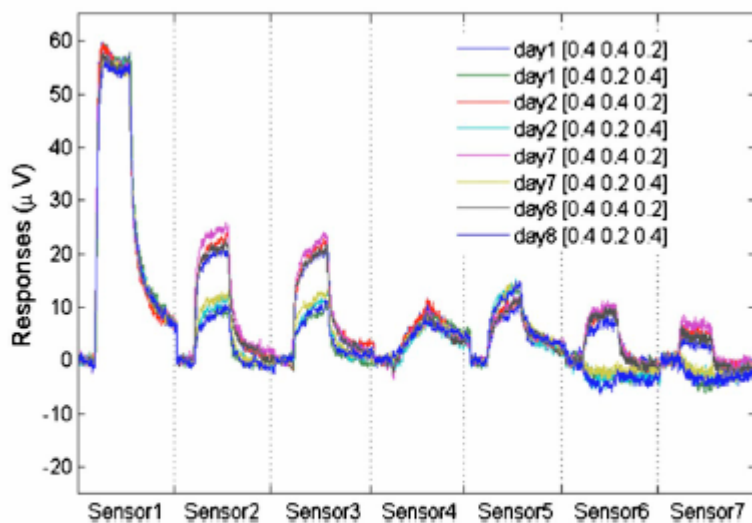


FIG. 4. (Color online) Comparison of the response patterns of two arbitrary compositions collected on different days to display the reproducibility of the responses.

TABLE I. Response data sets for DMMP-water-ethanol mixtures.

Set	Number of compositions	Number of patterns	Number of common compositions	Composition category
1	29	116	21	1
2	29	116	21	1
3	45	180	45	2
4	27	108	21	1
5	27	108	21	1
6	45	180	45	2

TABLE II. Response data sets for acetone-water-ethanol mixtures.

Set	Number of compositions	Number of patterns	Number of common compositions	Composition category
1	21	84	21	1
2	21	84	21	1

The experimental apparatus shown in Fig. 1 led to two features for vapor concentrations. First, there was a highest concentration for each of the three vapors due to the constant vapor temperature and flow rate of each of the vapor generators. Second, the sum of the three fractional concentrations was 100% due to the constant flow rate (50 SCCM) going through the flow cell and the same flow rate (50 SCCM) going through each of the three vapor generators. Because of the restriction of the second feature, the three-element composition vector had only two degrees of freedom.

If the component proportion represents the “odor” of a vapor mixture, the concentration scale of the mixture represents the strength of the odor. From Eq. (1), a mixture with certain odor can be expressed as

$$(c_1, c_2, c_3) = [(flow_1/flow_t)C_1, (flow_2/flow_t)C_2, (flow_3/flow_t)C_3] \quad (3)$$

There are only two independent variables to express the odor or the vector of  $(c_1, c_2, c_3)$ . In a three-dimensional space for all possible compositions of ternary mixtures, whose coordinates are expressed by the three fraction concentrations of  $F_{c_1}$ ,  $F_{c_2}$ , and  $F_{c_3}$ , all of the possible odors form an equilateral triangle surface (two dimensional (2D)) with three vertices of (100%, 0%, 0%), (0%, 100%, 0%), and (0%, 0%, 100%) due to the restriction of  $F_{c_1}+F_{c_2}+F_{c_3}=100\%$ .

For better recognition of the response patterns, the ANN needs to be more “experienced”; i.e., more data need to be used to train the ANN. We prepared the training data based on two major considerations: (1) By choosing mixture compositions representing a variety of odors, the apparatus allowed us to adjust the component concentrations at suitable increments and to provide detection vapor mixtures with compositions evenly covering many compositions or the odors on the triangle surface in the “concentration space” (see Fig. 5 later). These vapor compositions included individual vapors, binary mixtures, and ternary mixtures. Usually, we varied the component fraction concentration in a step of 20% by adjusting the flow rate of the second flow controller in steps of 10 SCCM for the total flow rate of 50 SCCM. (2) In repeated detection at a given composition, we

usually took four measurements per composition and these repeated measured patterns helped the network to be more experienced and, thus, to filter out the noise. The measurement software allowed us to set the number of pulses, pulse duration, and the time interval between a pulse and its succeeding pulse. In our experiments, the number of pulses, duration, and interval were 4, 30 s, and 150 s, respectively. We measured the different compositions one by one and recorded the data into a text-format (ASCII) data file. One such data file/set (20–30 MB) usually included data related to 21–45 mixtures and took 5–10 h for the data collection.

## **E. Artificial neural network training and testing**

We chose an ANN for pattern recognition, since most responses of the microcantilevers were nonlinear and complex. The biologically inspired ANN is a self-adapting system that can modify its response to external forces by using previous experience, which offers a more flexible and faster method of analysis.<sup>24</sup> The ANN we used for the pattern recognition was a back-propagation ANN written in MATLAB®. The training procedure and testing details will be discussed elsewhere.<sup>28</sup>

## **III. RESULTS AND DISCUSSION**

### **A. Response patterns**

The successful identification of vapor mixture by using electronic nose depended on the sensor array responses to different mixtures with different patterns. For vapor mixtures with the same components but different component proportions, the mixtures can be labeled as having different odors. If a sensor array responded with different patterns to different odors, the electronic nose could discriminate different odors or component proportions. Therefore, in addition to identifying the presence or absence of certain components, we can also quantify the concentrations of the components. As shown in Fig. 2, the microcantilever array responded to different compositions with different response patterns.

For better pattern recognition, we also needed low level of noise and good reproducibility of the responses, in addition to high level of difference between patterns for different compositions. Some example response patterns from our data are shown in Fig. 3. Figure 3(a) shows the response patterns obtained for single pulses at varying concentrations for binary mixtures of DMMP and water vapor; response patterns with four repeated pulses for the same DMMP-water binary mixtures are shown in Fig. 3(b). Figures 3(a) and 3(b) graphically display the levels of the noise and the reproducibility comparing the difference between patterns corresponding to varying compositions. The repeated responses had been used to train the ANN to make it more experienced with the features of noise and signal. Figure 3(c) shows the patterns for ethanol-DMMP binary mixtures at varying concentrations, and Fig. 3(d) shows the patterns of the DMMP, water, and ethanol ternary mixtures. From these examples, it is clear that the difference between patterns of different pulse to the same composition is somewhat smaller compared to the difference between the patterns corresponding to two different compositions and that the reproducibility is good.

Besides the reproducibility of consecutive pulses, we also monitored the reproducibility between patterns to the same composition but collected in different days. As shown in Fig. 4, two ternary mixtures were measured in four different days in an 8 day period. Figure 4 shows that the patterns measured in different days changed a little and quite smaller than the pattern difference among different compositions. The pattern reproducibility of the sensor array over several days guarantees that the electronic nose trained by using data of 1 day will be able to correctly detect mixtures presented to it several days later. Even though our study was limited to a 2 week period, it should be good for a longer period. We plan to test over longer periods in the next study.

## B. Comparison of the predicted concentrations to the actual concentrations

As we discussed in Sec. II D, all possible odors ( $F_{c_1}, F_{c_2}, F_{c_3}$ ) form a triangular surface in the “concentration space,” which is the space of all possible compositions. If we need the ANN to be representatively trained over the whole triangular surface, we need to accordingly collect training data over the triangle surface. We collected such data for DWE mixtures in six different days corresponding to six data sets (Table I). The six data sets were in two categories: four data sets with about 25 different mixtures and two data sets with 45 mixtures, each of which was different from any of the first category. We trained and tested the ANN by using several different methods: (1) one data set of the first category was used for training and other five for testing; (2) all data were placed in one pool and randomly selected 80% for training and 20% for testing. We collected data on AWE mixtures in two different days (Table II). The two data sets correlate to 21 compositions. For both DWE and AWE mixtures, we trained the ANN by using the above two methods by dividing the data into two groups for training and testing.

In the restricted composition space (the 2D triangle surface), one point represents a composition. Figure 5 graphically compares the predicted compositions (stars) with the actual compositions (filled circles) for the DWE mixtures. Figure 5(a) displays the predicted values of the first category mixtures, and Fig. 5(b) displays the predicted values of the second category mixtures. The predicted concentrations are quite close to the actual values. Figure 5(b) shows that the ANN can also predict mixture compositions that are different from compositions used for training.

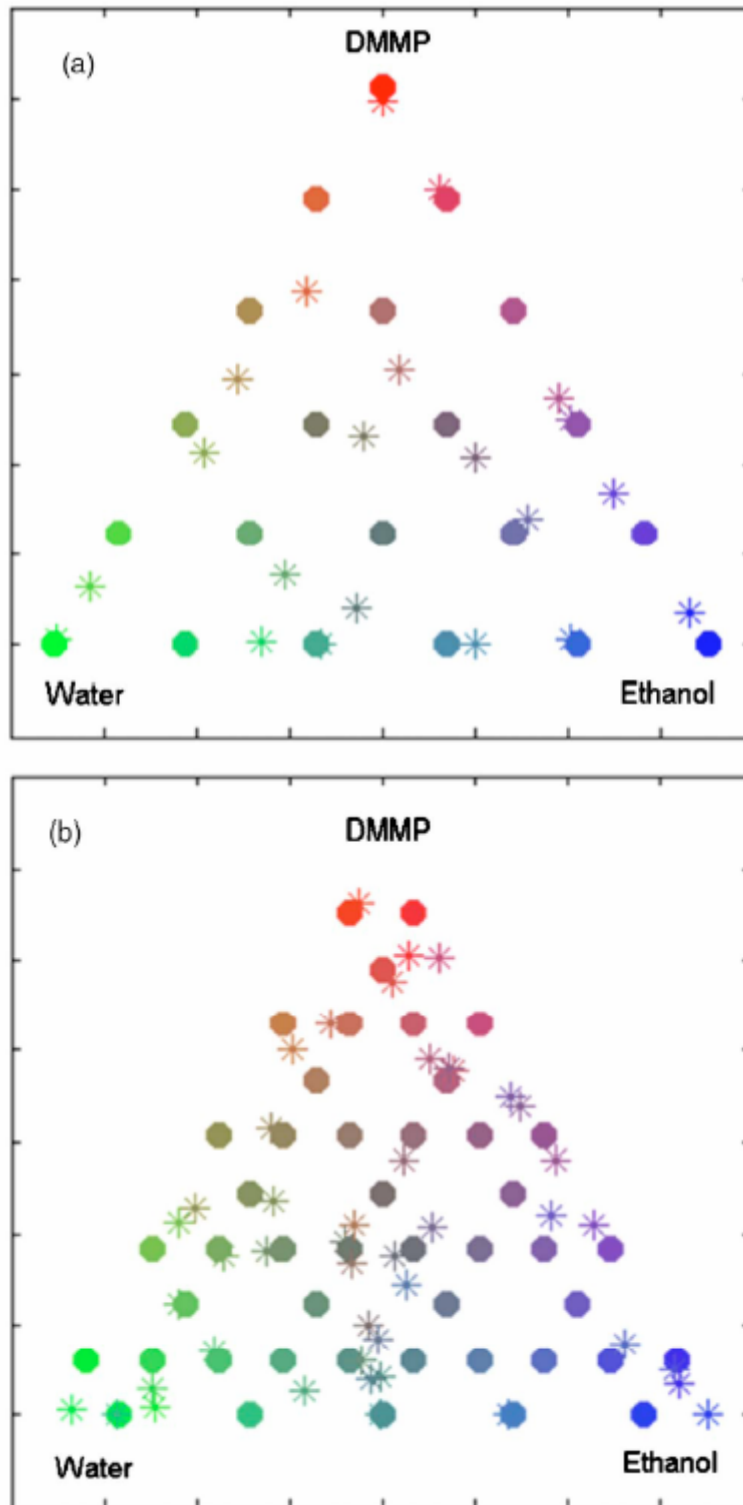


FIG. 5. (Color online) Graphical comparison of the predicted and actual compositions. The triangle is the 2D surface for all of the possible compositions  $([F_{c_1}F_{c_2}F_{c_3}], \text{i.e., } 1.0 \geq F_{c_1}, F_{c_2}, F_{c_3} \geq 0.0_ \text{ with the restriction } F_{c_1} + F_{c_2} + F_{c_3} = 1)$ . One dot represents an actual composition and one star represents an estimated composition. The color of a dot or star is a mixture of three individual colors of red (DMMP), green (water), and blue (ethanol) with the same proportion of the dot's or star's composition.

TABLE III. Prediction results for data set 5 of DMMP-water-ethanol mixtures. Note:  $D$ =DMMP,  $W$ =water, and  $E$ =ethanol.

Actual composition			Predicted composition		
$D$	$W$	$E$	$D$	$W$	$E$
1.00	0.00	0.00	0.98	0.01	0.01
0.80	0.20	0.00	0.83	0.16	0.01
0.80	0.00	0.20	0.78	0.03	0.19
0.60	0.40	0.00	0.62	0.33	0.05
0.60	0.20	0.20	0.57	0.18	0.25
0.60	0.00	0.40	0.47	0.04	0.49
0.40	0.60	0.00	0.35	0.61	0.04
0.40	0.40	0.20	0.36	0.41	0.24
0.40	0.20	0.40	0.38	0.20	0.42
0.40	0.00	0.60	0.34	0.03	0.62
0.20	0.80	0.00	0.20	0.77	0.02
0.20	0.60	0.20	0.22	0.64	0.14
0.20	0.40	0.40	0.18	0.42	0.40
0.20	0.20	0.60	0.23	0.12	0.65
0.20	0.00	0.80	0.13	0.02	0.85
0.00	1.00	0.00	0.00	0.95	0.04
0.00	0.80	0.20	0.00	0.84	0.16
0.00	0.60	0.40	0.00	0.61	0.38
0.00	0.40	0.60	0.01	0.39	0.60
0.00	0.20	0.80	0.01	0.07	0.92
0.00	0.00	1.00	0.00	0.01	0.99
0.04	0.96	0.00	0.00	0.99	0.01
0.04	0.76	0.20	0.05	0.75	0.21
0.04	0.56	0.40	0.00	0.57	0.42
0.04	0.36	0.60	0.04	0.30	0.66
0.04	0.16	0.80	0.03	0.05	0.91
0.04	0.00	0.96	0.05	0.00	0.95

TABLE IV. Prediction results for data set 6 of DMMP-water-ethanol mixtures. Note:  $D$ =DMMP,  $W$ =water, and  $E$ =ethanol.

Actual composition			Predicted composition		
$D$	$W$	$E$	$D$	$W$	$E$
0.90	0.00	0.10	0.82	0.03	0.16
0.70	0.30	0.00	0.78	0.18	0.04
0.70	0.20	0.10	0.66	0.18	0.16
0.70	0.10	0.20	0.54	0.12	0.34
0.70	0.00	0.30	0.62	0.03	0.35
0.50	0.50	0.00	0.43	0.55	0.02
0.50	0.40	0.10	0.39	0.45	0.15
0.50	0.30	0.20	0.65	0.25	0.11
0.50	0.20	0.30	0.54	0.17	0.29
0.50	0.10	0.40	0.37	0.07	0.56
0.50	0.00	0.50	0.47	0.04	0.49
0.30	0.70	0.00	0.32	0.66	0.02
0.30	0.60	0.10	0.22	0.62	0.15
0.30	0.50	0.20	0.36	0.43	0.21
0.30	0.40	0.30	0.25	0.44	0.31
0.30	0.30	0.40	0.28	0.31	0.42
0.30	0.20	0.50	0.24	0.12	0.64
0.30	0.10	0.60	0.27	0.11	0.62
0.30	0.00	0.70	0.18	0.03	0.79
0.10	0.90	0.00	0.01	0.97	0.02
0.10	0.80	0.10	0.06	0.87	0.08
0.10	0.70	0.20	0.04	0.84	0.12
0.10	0.60	0.30	0.10	0.63	0.27
0.10	0.50	0.40	0.08	0.64	0.28
0.10	0.40	0.50	0.16	0.37	0.47
0.10	0.30	0.60	0.06	0.43	0.51
0.10	0.20	0.70	0.11	0.12	0.77
0.10	0.10	0.80	0.09	0.09	0.82
0.10	0.00	0.90	0.06	0.00	0.94
0.80	0.10	0.10	0.69	0.12	0.19
0.60	0.30	0.10	0.50	0.36	0.14
0.60	0.10	0.30	0.48	0.07	0.44
0.40	0.50	0.10	0.22	0.62	0.15
0.40	0.30	0.30	0.23	0.49	0.28
0.40	0.10	0.50	0.24	0.12	0.64
0.20	0.70	0.10	0.07	0.87	0.05
0.20	0.50	0.30	0.21	0.66	0.12
0.20	0.30	0.50	0.11	0.44	0.46
0.20	0.10	0.70	0.10	0.11	0.78
0.00	0.90	0.10	0.00	0.98	0.02
0.00	0.70	0.30	0.00	0.87	0.13
0.00	0.50	0.50	0.00	0.61	0.39
0.00	0.30	0.70	0.02	0.30	0.68
0.00	0.10	0.90	0.00	0.01	0.99

### C. Prediction of the mixtures of DMMP, water, and ethanol

For the DMMP-water-ethanol mixtures, we trained the ANN by using data set 2 of Table I. The data set correlates to 29 different compositions including 3 individual vapors, 16 binary mixtures, and 10 ternary mixtures. There are 21 common compositions in data set 2 with those in the data sets 1, 4 and 5. The common compositions are the first 21 compositions in Table III. The 29 compositions cover all of the 2D composition space (the triangle surface of Fig. 5). We tested the trained ANN by using other five data sets. The tests on data sets 5 and 6 are shown in Tables III and IV, respectively. Note that the data set 6 has no common compositions with the data set 2, which was used for training. Comparing the test results in Tables III and IV, there is no obvious difference in prediction accuracy between the tests of the two data sets. The ANN can recognize patterns correlating to compositions that are not the compositions used for training.

TABLE V. Summary of prediction errors for DMMP-water-ethanol mixtures. Note: cat. =category. Refer to Table I.

Data set		DMMP	Water	Ethanol	Average
1 (cat. 1)	Mean	0.0069	-0.0287	0.0218	0.0000
	MSE	0.0035	0.0041	0.0031	0.0036
	Max	0.1360	0.1110	0.1218	0.1229
	Min	-0.1497	-0.1295	-0.1710	-0.1501
4 (cat. 1)	Mean	-0.0099	0.0214	-0.0115	0.0000
	MSE	0.0048	0.0055	0.0065	0.0056
	Max	0.1766	0.2050	0.1525	0.1780
	Min	-0.1752	-0.1281	-0.2082	-0.1705
5 (cat. 1)	Mean	-0.0143	-0.0108	0.0251	0.0000
	MSE	0.0014	0.0021	0.0023	0.0019
	Max	0.0329	0.0414	0.1195	0.0646
	Min	-0.1285	-0.1287	-0.0606	-0.1060
3 (cat. 2)	Mean	-0.0508	0.0552	-0.0044	0.0000
	MSE	0.0078	0.0087	0.0068	0.0078
	Max	0.0908	0.1890	0.1609	0.1469
	Min	-0.1805	-0.0813	-0.1936	-0.1518
6 (cat. 2)	Mean	-0.0441	0.0317	0.0124	0.0000
	MSE	0.0070	0.0069	0.0064	0.0068
	Max	0.1452	0.1890	0.1599	0.1647
	Min	-0.1760	-0.1206	-0.1759	-0.1575

TABLE VI. Prediction results for data set 2 of acetone-water-ethanol mixtures. Note:  $A$ =acetone,  $W$ =water, and  $E$ =ethanol.

Actual composition			Predicted composition		
$A$	$W$	$E$	$A$	$W$	$E$
1.00	0.00	0.00	0.96	0.03	0.01
0.80	0.20	0.00	0.85	0.15	0.00
0.80	0.00	0.20	0.86	0.03	0.11
0.60	0.40	0.00	0.67	0.32	0.02
0.60	0.20	0.20	0.69	0.21	0.10
0.60	0.00	0.40	0.52	0.07	0.41
0.40	0.60	0.00	0.32	0.54	0.13
0.40	0.40	0.20	0.55	0.34	0.11
0.40	0.20	0.40	0.56	0.13	0.30
0.40	0.00	0.60	0.54	0.05	0.41
0.20	0.80	0.00	0.35	0.63	0.02
0.20	0.60	0.20	0.19	0.58	0.23
0.20	0.40	0.40	0.24	0.30	0.46
0.20	0.20	0.60	0.57	0.07	0.37
0.20	0.00	0.80	0.19	0.02	0.79
0.00	1.00	0.00	0.00	0.99	0.01
0.00	0.80	0.20	0.08	0.61	0.31
0.00	0.60	0.40	0.03	0.45	0.52
0.00	0.40	0.60	0.03	0.31	0.66
0.00	0.20	0.80	0.16	0.13	0.72
0.00	0.00	1.00	0.04	0.01	0.95

A summary of the five tested data sets is displayed in Table V. The average errors for each of the three components are very small, which are  $<0.06$ . In our ANN training, the mean square error (MSE) was used as the network performance error. During training, the weights and biases were iteratively adjusted to minimize the MSE. In general, the MSE is a measure of the accuracy of ANN predictions. The MSEs in Table V have not shown any obvious trend to increase with the time delay between collections of data for testing and data for training. The MSE of data set 4 (seventh day) is bigger than the MSE of data set 1 (first day), ( $0.0056 > 0.0036$ ), but the MSE of 5 (eighth day) is smaller ( $0.0019$ ). Compared to data sets 1, 4, and 5, which have 21 common compositions with the trained data set 2, the test MSEs of data sets 3 and 6 ( $0.0078$  and  $0.0068$ ) are obviously bigger. We ascribe the bigger MSEs to the tested compositions being not exactly equal to the compositions that were trained. The network recognized the patterns of those interpolated compositions as patterns similar to those trained patterns and was able to output approximate compositions.

Based on the predicted compositions as those shown in Tables III and IV, we can identify and quantify individual components from the ternary mixtures. For example, we set DMMP as the interested vapor and water and ethanol as the interference vapors. For identification, our goal is to predict the presence or absence of the DMMP. From Tables III and IV, we find that the highest predicted concentration for zero DMMP was  $0.02$ . If we set  $0.03$  ( $\sim 3$  ppb) as the criterion to alarm for the presence of DMMP, we find that there is no false alarm for any of the 11 cases of DMMP absence (i.e., zero false positive). However, for the 61 cases of DMMP presence in Tables III and IV, there are 3 cases without alarm that are expected to alarm ( $3/61$  chance of false negative). They are  $[0.04\ 0.96\ 0.00]$  and  $[0.04\ 0.56\ 0.40]$  in Table III and  $[0.10\ 0.90\ 0.00]$  in Table IV. If we restrict our discussion only to the data in Tables III and IV, the presence or absence of DMMP is 100% reliable for DMMP concentration more than  $0.20$  ( $\sim 20$  ppb) and 95% reliable for concentration between  $0.20$  and  $0.0$ . For component quantification, the average error on component concentration is below  $0.05$  (or 5%, Table VI), except in data set 3 where the average errors are  $0.051$  and  $0.055$  for DMMP and water, respectively.

Unlike the analytical chemistry approach that individually detects the components and then allows us to calculate the composition of the mixture, the electronic nose approach directly detects the mixture (by recognizing the unique response pattern correlated with a mixture) and simultaneously allows us to calculate the component concentrations. The ANN-predicted concentrations of DMMP from all of the measurements in the five tested data sets are shown in Fig. 6(a) these data come from the two possible binary mixtures and the ternary mixtures. Similarly, the predicted concentrations for water and ethanol are shown in Figs. 6(b) and 6(c), respectively. Finally, all of the data are summarized in Fig. 7.

In former paragraphs, we usually present the prediction results in a three-element vector (such as those in Tables III and IV). To change an angle to look at the data, we rearranged the order to list the results, which was not according to the mixture composition (vector) but to the components (elements). The links among the three component concentrations in a vector were ignored and we focused on one component each time. Take DMMP as an example; we put together all predicted compositions with the same DMMP concentration no matter what the ratio of other two concentrations of water or ethanol was. Thus, based on the test results of the five tested data sets, we got the predicted concentrations ( $0.0-1.0$ ) for DMMP vapor within the mixtures that concentration proportion of other two components was not restricted, as shown in Fig. 6(a). Similarly, we also got the predicted concentrations for water and ethanol, as shown in Figs. 6(b) and 6(c), respectively. To save space, we put the three prediction curves into the one frame of graph (Fig. 7).

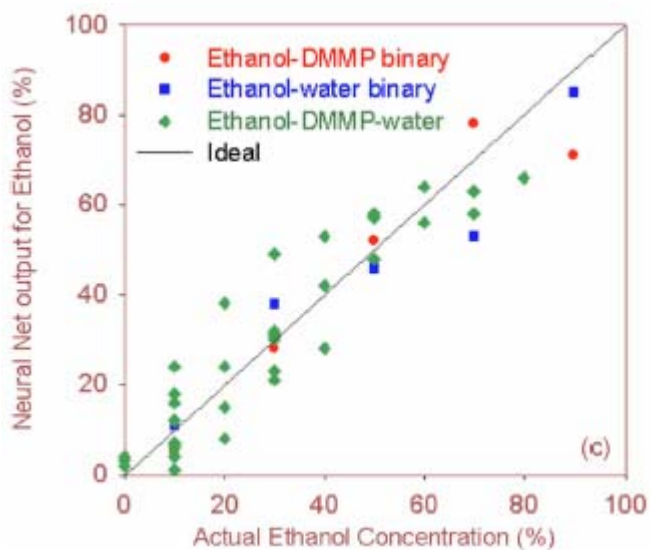
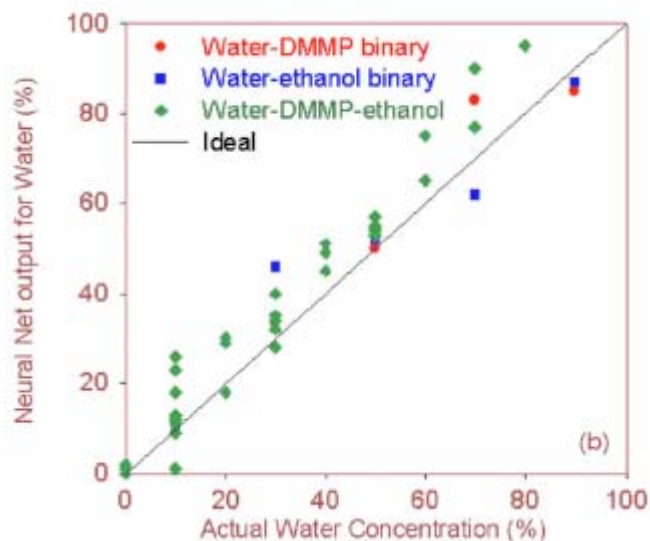
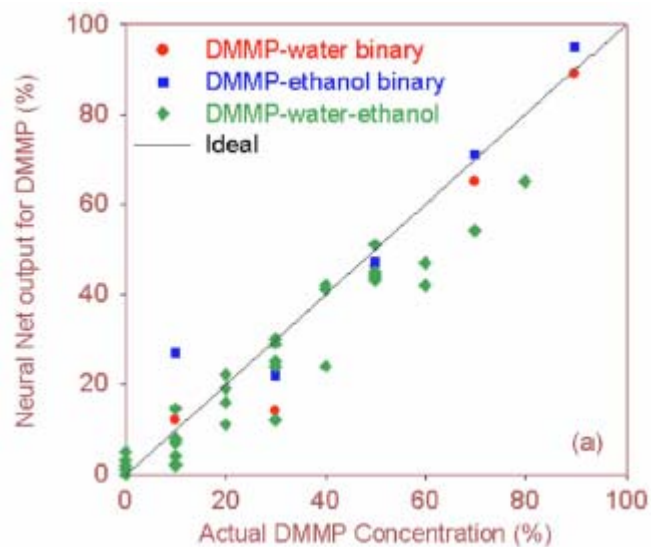


FIG. 6. (Color online) Comparison of the estimated concentrations of (a) DMMP vapor, (b) water vapor, and (c) ethanol vapor, with the actual concentrations that were presented to the sensor array for a single test data set. The data consisted of those for binary mixtures (15 mixtures) and ternary mixtures (30 mixtures), where the mixture compositions were different from the compositions of mixtures used in the training set. Please note that 100% of actual concentrations for DMMP, water, and ethanol vapors from the vapor generators are 100 ppb, 60 ppm, and 60 ppm, respectively.

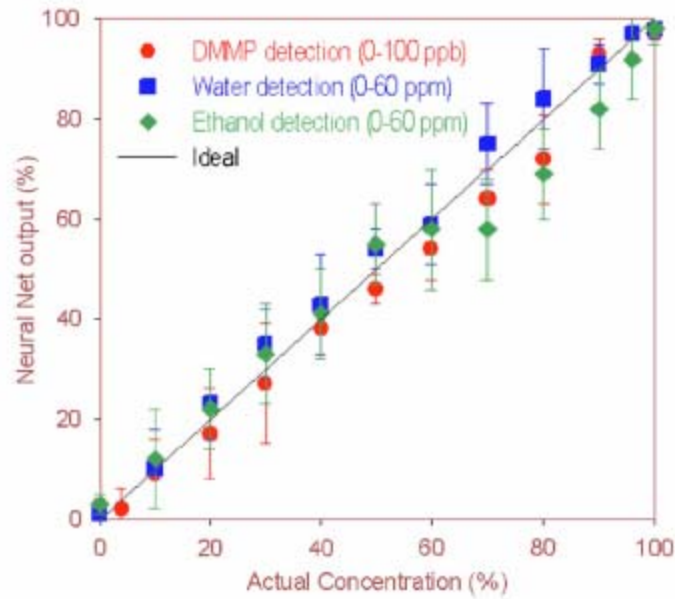


FIG. 7. (Color online) Comparison of the estimated concentrations of DMMP, water, and ethanol vapors, with the actual concentrations that were presented to the sensor array. The data shown are from all five test data sets taken over the 2 week period. For concentrations over 70%, each point was the average of four to eight data points; for concentrations in the range of 30%–60%, each point was averaged over 10–20 data points; for concentrations in the range of 0%–20%, each point was averaged over 24–30 data points. There were 9 mixtures for unitary, 72 mixtures for binary, and 92 mixtures for ternary mixtures. So, the bulk of the data taken was for ternary mixtures where all three component vapors had nonzero concentrations.

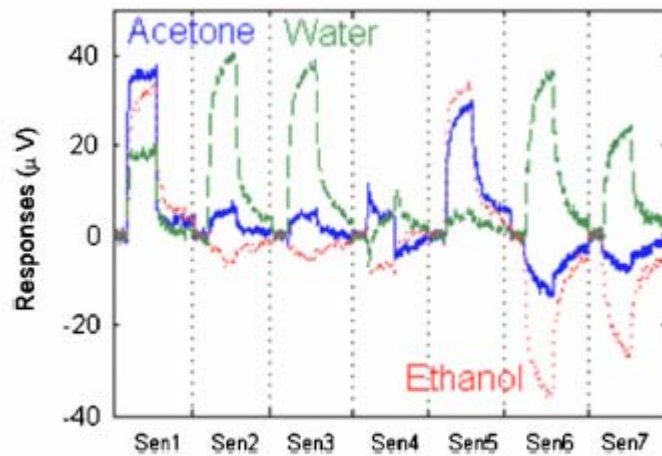


FIG. 8. (Color online) Response patterns of individual acetone, water, and ethanol vapors.

For lower concentrations ( $\sim 0.0$ ), there were usually more mixture vapors detected. For DMMP concentration of 0.10, there were 24 mixtures detected, and the prediction mean and error were calculated based on the prediction results of the 24 mixtures. The results in Fig. 7 show that the electronic nose system in this report, which includes the seven-pair microcantilever array and the

neural network algorithm, is capable of selectively detecting DMMP vapor of ppb concentration in the presence of two interference vapors of ppm concentrations.

#### D. Prediction of the mixtures of acetone, water, and ethanol

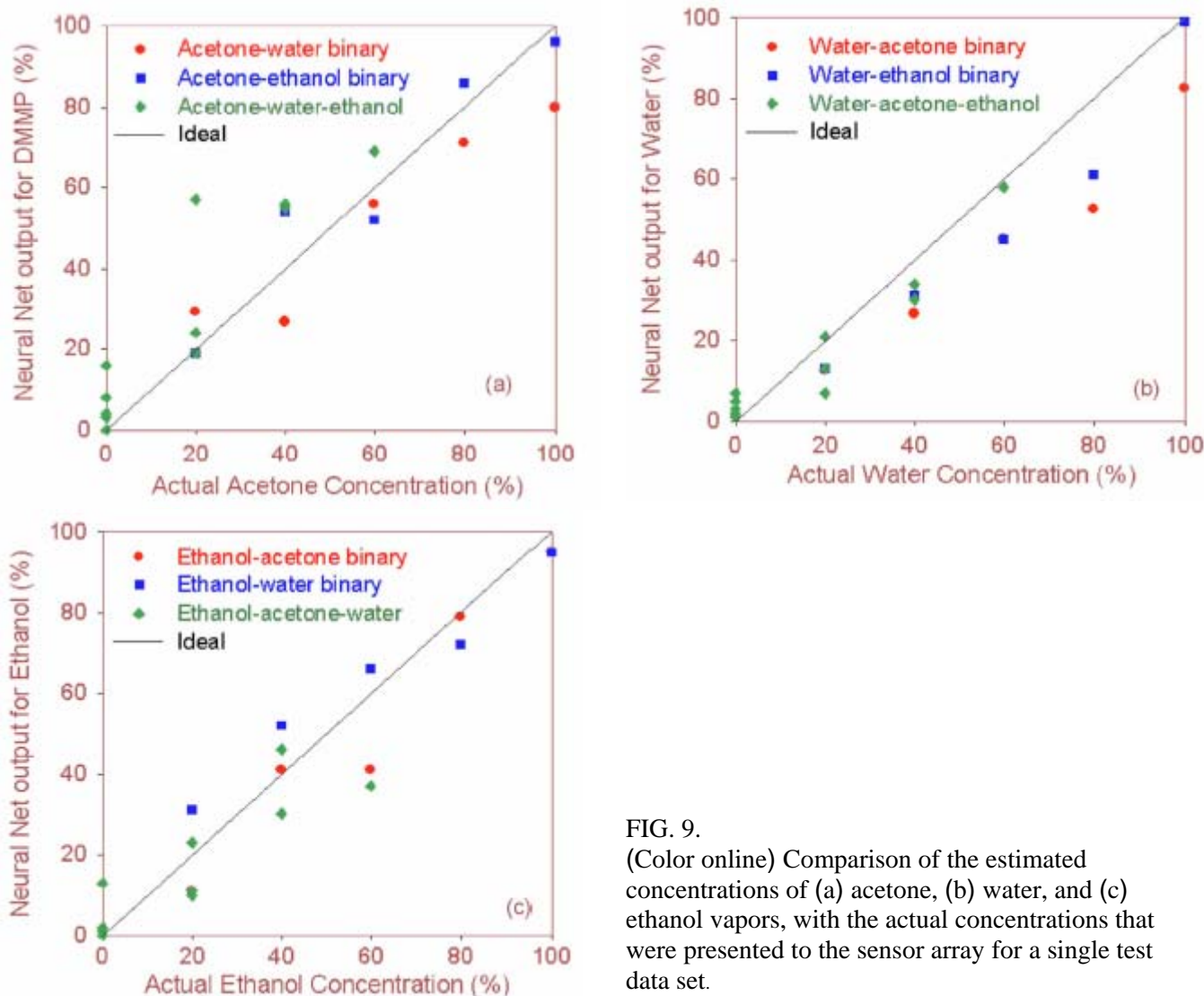


FIG. 9. (Color online) Comparison of the estimated concentrations of (a) acetone, (b) water, and (c) ethanol vapors, with the actual concentrations that were presented to the sensor array for a single test data set.

To use the same microcantilever array, we also studied the detection of ternary mixture of acetone, water, and ethanol. The response patterns for the three individual vapors are shown in Fig. 8. The response pattern of acetone is more similar to the pattern of ethanol comparing with the pattern of water. The biggest difference between the patterns of acetone and ethanol is at sensors 6 and 7.

We collected two data sets in two different days which was 6 days apart. Each data set includes the response patterns to 21 different compositions (as those top 21 compositions in Table III), which fraction concentrations were adjusted in a step of 0.20. Each of the 21 different compositions or

mixture vapors was measured in four pulses (30 s pulse duration and 150 s interval). One data set

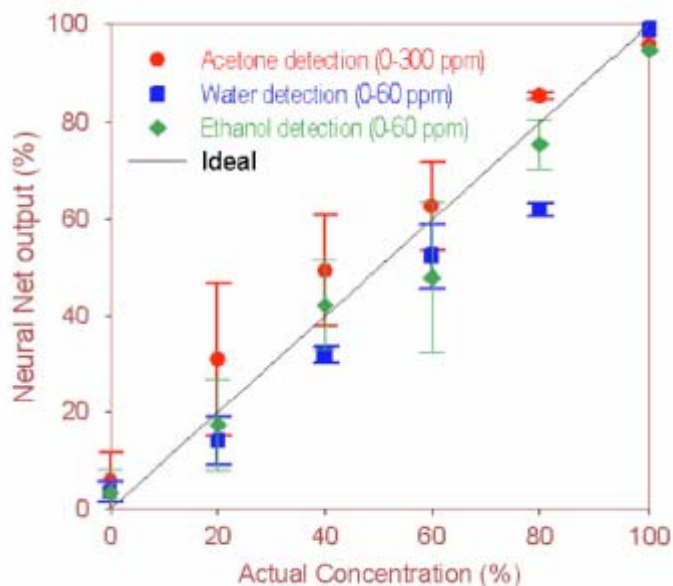


FIG. 10. (Color online) Comparison of the average estimated concentrations of acetone, water, and ethanol vapors, with the actual concentrations that were presented to the sensor array. The data shown are from one test data set taken over the 1 week period (or 5 days apart from the date to take the data set for training).

was used to train the ANN, and the other was used to test the training. The predicted compositions are shown in Table VI and the graphical prediction results are shown in Figs. 9 and 10. The prediction results of the electronic nose system on the acetone-water-ethanol mixtures were still good but not as good as the prediction on the DMMP-water-ethanol mixtures. The errors of the predicted concentrations were less than 0.20 except the composition of [0.20 0.20 0.60]. For each of the three vapors, the presence (concentrations of >0.20) and absence (concentration of 0.0) were easy to discriminate because the predicted value of actual concentration bigger than 0.20 was always bigger than the predicted value of actual concentration that is 0.

The average MSEs for acetone, water, and ethanol were 0.0080, 0.0071, and 0.0067, respectively (we skipped the composition of [0.20 0.20 0.60]). Compared to the MSEs in Table V, the MSEs of the acetone-water-ethanol mixtures are bigger than the MSEs of the DMMP-water-ethanol mixtures with the same compositions as those for training the network (data sets 1, 4, and 5 in Table V).

Considering the similar response patterns of acetone and ethanol, the pattern recognition of the acetone-water-ethanol mixture responses must be more difficult than that of the DMMP-water-ethanol mixture responses. Reproducibility of vapor concentrations together with the reproducible responses from the microcantilevers were necessary for the training of the ANN to be effective over long time periods.

#### IV. SUMMARY

We have investigated selective detection of components in ternary vapor mixtures of DMMP-water-ethanol and acetone-water-ethanol by using an electronic nose system based on a microcantilever sensor array and an ANN maximum concentration of DMMP that was 100 ppb, and the concentrations of the other vapors were in the ppm range. Once the neural network was trained with a training vapor mixture set, the trained neural network was able to quantitatively identify either the

individual vapors or the components of binary and ternary mixtures within the 2 week period of the experiments. The neural network was able to quantify the vapor concentrations within 20% and was able to detect DMMP with zero false alarm rate at 10 ppb level. Stable sensor coatings providing reproducible signals together with well-calibrated vapor streams are necessary to conduct such vapor detection studies. The SAM coatings that we used were covalently bound to the microcantilever surface and are expected to be only a monolayer thick; this leads to robust, durable coatings with reproducible responses. Further studies are underway to improve the sensor array (by adding more sensors/coatings) and also to incorporate a preconcentrator so that more complex vapor mixtures could be analyzed.

## ACKNOWLEDGMENTS

These studies were conducted with the support from Office of Naval Research (ONR) Contract No. N00014-06-C- 0182 to Triton Systems, Inc., and Contract No. N00014-06- IP-20082 to Oak Ridge National Laboratory (ORNL). ORNL is operated and managed by UT-Battelle, LLC for the U.S. Department of Energy under Contract No. DE-AC05- 00OR22725.

## FOOTNOTES

- <sup>1</sup> K. Persaud and G. H. Dodd, *Nature (London)* **299**, 352 (1982).
- <sup>2</sup> B. Malnic, J. Hirono, T. Sato, and L. B. Buck, *Cell* **96**, 713 (1999).
- <sup>3</sup> R. Axel, *Angew. Chem. Int. Ed.* **44**, 6110 (2005).
- <sup>4</sup> A. Hierlemann and H. Baltes, *Analyst (Cambridge, U.K.)* **128**, 15 (2003).
- <sup>5</sup> G. Muller, P. P. Deimel, W. Hellmich, and C. Wagner, *Thin Solid Films* **296**, 157 (1997).
- <sup>6</sup> K. J. Albert, N. S. Lewis, C. L. Schauer, G. A. Sotzing, S. E. Stitzel, T. P. Vaid, and D. R. Walt, *Chem. Rev. (Washington, D.C.)* **100**, 2595 (2000).
- <sup>7</sup> D. James, S. M. Scott, Z. Ali, and W. T. O'Hare, *Mikrochim. Acta* **149**, 1 (2005).
- <sup>8</sup> T. C. Pearce, S. S. Schffman, H. T. Nagle, and J. W. Gardner, *Handbook of Machine Olfaction* (Wiley-VCH, Weinheim, 2003).
- <sup>9</sup> L. A. Pinnaduwege, H. F. Ji, and T. Thundat, *IEEE Sens. J.* **5**, 774 (2005).
- <sup>10</sup> R. Archibald, P. Datskos, G. Devault, V. Lamberti, N. Lavrik, D. Noid, and M. D. P. Sepaniak, *Anal. Chim. Acta* **584**, 101 (2007).
- <sup>11</sup> N. T. Greene and K. D. Shimizu, *J. Am. Chem. Soc.* **127**, 5695 (2005).
- <sup>12</sup> M. D. Hsieh and E. T. Zellers, *J. Occup. Environ. Hyg.* **1**, 149 (2004).
- <sup>13</sup> M. D. Hsieh and E. T. Zellers, *Anal. Chem.* **76**, 1885 (2004).
- <sup>14</sup> M. Penza, G. Cassano, and F. Tortorella, *Meas. Sci. Technol.* **13**, 846 (2002).
- <sup>15</sup> L. R. Senesac, P. Dutta, P. G. Datskos, and M. J. Sepaniak, *Anal. Chim. Acta* **558**, 94 (2006).

- <sup>16</sup> D. Then, A. Vidic, and Ch. Ziegler, *Sens. Actuators B* **117**, 1 (2006).
- <sup>17</sup> T. Gao, M. D. Woodka, B. S. Brunschwig, and N. S. Lewis, *Chem. Mater.* **18**, 5193 (2006).
- <sup>18</sup> K. J. Albert, D. R. Walt, D. S. Gill, and T. C. Pearce, *Anal. Chem.* **73**, 2501 (2001).
- <sup>19</sup> F. M. Battiston, J. P. Ramseyer, H. P. Lang, M. K. Baller, C. Gerber, J. K. Gimzewski, E. Meyer, and H. J. Guntherodt, *Sens. Actuators B* **77**, 122 (2001).
- <sup>20</sup> *Handbook of Machine Olfaction*, edited by T. Pearce, S. Schiffman, H. Nagle, and J. Gardner (Wiley-VCH, Weinheim, Germany, 2003).
- <sup>21</sup> P. C. Jurs, G. A. Bakken, and H. E. McClelland, *Chem. Rev. (Washington, D.C.)* **100**, 2649 (2000).
- <sup>22</sup> S. M. Scott, D. James, and Z. Ali, *Mikrochim. Acta* **156**, 183 (2006).
- <sup>23</sup> A. B. Chelani, C. V. C. Rao, K. M. Phadke, and M. Z. Hasan, *Environ. Modell. Software* **17**, 159 (2002).
- <sup>24</sup> J. H. Sohn, R. Smith, E. Yoong, J. H. Leis, and G. Galvin, *Biosyst. Eng.* **86**, 399 (2003).
- <sup>25</sup> L. A. Pinnaduwege, W. Zhao, A. C. Gehl, S. L. Allman, A. Shepp, K. K. Mahmud, and J. H. Leis, *Appl. Phys. Lett.* **91**, 044105 (2007).
- <sup>26</sup> L. A. Pinnaduwege, A. C. Gehl, S. L. Allman, A. Johansson, and A. Boisen, *Rev. Sci. Instrum.* **78**, 055101 (2007).
- <sup>27</sup> L. A. Pinnaduwege, D. L. Hedden, A. Gehl, V. Boiadjev, J. E. Hawk, R. H. Farahi, T. Thundat, E. J. Houser, S. Stepnowski, R. A. McGill, L. Deel, and R. T. Lareau, *Rev. Sci. Instrum.* **75**, 4554 (2004).
- <sup>28</sup> J. H. Leis, W. Zhao, L. A. Pinnaduwege, A. C. Gehl, S. L. Allman, A. Shepp, and K. K. Mahmud, *IEEE Sens. Lett.* (submitted).